

## Isospin Mixing in $^{80}\text{Zr}$ : From Finite to Zero Temperature

S. Ceruti,<sup>1,2</sup> F. Camera,<sup>1,2</sup> A. Bracco,<sup>1,2</sup> R. Avigo,<sup>1,2</sup> G. Benzoni,<sup>2</sup> N. Blasi,<sup>2</sup> G. Bocchi,<sup>1,2</sup> S. Bottoni,<sup>1,2</sup> S. Brambilla,<sup>2</sup> F. C. L. Crespi,<sup>1,2</sup> A. Giaz,<sup>2</sup> S. Leoni,<sup>1,2</sup> A. Mentana,<sup>1,2</sup> B. Million,<sup>2</sup> A. I. Morales,<sup>1,2</sup> R. Nicolini,<sup>1,2</sup> L. Pellegrini,<sup>1,2</sup> A. Pullia,<sup>1,2</sup> S. Riboldi,<sup>1,2</sup> O. Wieland,<sup>2</sup> B. Birkenbach,<sup>3</sup> D. Bazzacco,<sup>4</sup> M. Ciemala,<sup>5</sup> P. Désesquelles,<sup>6</sup> J. Eberth,<sup>3</sup> E. Farnea,<sup>4</sup> A. Gørgen,<sup>7,8</sup> A. Gottardo,<sup>9,10</sup> H. Hess,<sup>3</sup> D. S. Judson,<sup>11</sup> A. Jungclaus,<sup>12</sup> M. Kmiecik,<sup>5</sup> W. Korten,<sup>7</sup> A. Maj,<sup>5</sup> R. Menegazzo,<sup>4</sup> D. Mengoni,<sup>9,4</sup> C. Michelagnoli,<sup>9,4</sup> V. Modamio,<sup>10</sup> D. Montanari,<sup>9,4</sup> S. Myalski,<sup>5</sup> D. Napoli,<sup>10</sup> B. Quintana,<sup>13</sup> P. Reiter,<sup>3</sup> F. Recchia,<sup>9,4</sup> D. Rosso,<sup>10</sup> E. Sahin,<sup>10,8</sup> M. D. Salsac,<sup>7</sup> P.-A. Söderström,<sup>14,\*</sup> O. Stezowski,<sup>15</sup> Ch. Theisen,<sup>7</sup> C. Ur,<sup>4</sup> J. J. Valiente-Dobón,<sup>10</sup> and M. Zieblinski<sup>5</sup>

<sup>1</sup>*Dipartimento di Fisica dell'Università degli Studi di Milano, I-20133 Milano, Italy*

<sup>2</sup>*INFN, Sezione di Milano, I-20133 Milano, Italy*

<sup>3</sup>*Institut für Kernphysik, Universität zu Köln, Zùlpicher Straße 77, D-50937 Köln, Germany*

<sup>4</sup>*INFN, Sezione di Padova, I-35131 Padova, Italy*

<sup>5</sup>*Institute of Nuclear Physics, Polish Academy of Sciences, 31-342 Krakow, Poland*

<sup>6</sup>*CSNSM, CNRS/IN2P3 and Univ. Paris-Sud, F-91405 Orsay Campus, France*

<sup>7</sup>*IRFU, CEA/DSM, Centre CEA de Saclay, F-91191 Gif-sur-Yvette Cedex, France*

<sup>8</sup>*Department of Physics, University of Oslo, P.O. Box 1048 Blindern, N-0316 Oslo, Norway*

<sup>9</sup>*Dipartimento di Fisica dell'Università degli Studi di Padova, I-35131 Padova, Italy*

<sup>10</sup>*INFN, Laboratori Nazionali di Legnaro, Legnaro I-35020, Italy*

<sup>11</sup>*Oliver Lodge Laboratory, The University of Liverpool, Liverpool L69 7ZE, United Kingdom*

<sup>12</sup>*Instituto de Estructura de la Materia, CSIC, Madrid, E-28006 Madrid, Spain*

<sup>13</sup>*Laboratorio de Radiaciones Ionizantes, Universidad de Salamanca, E-37008 Salamanca, Spain*

<sup>14</sup>*Department of Physics and Astronomy, Uppsala University, SE-75120 Uppsala, Sweden*

<sup>15</sup>*Université Lyon 1, CNRS, IN2P3, Inst Phys Nucl Lyon, F-69622 Villeurbanne, France*

(Received 26 March 2015; revised manuscript received 12 July 2015; published 25 November 2015)

The isospin mixing was deduced in the compound nucleus  $^{80}\text{Zr}$  at an excitation energy of  $E^* = 54$  MeV from the  $\gamma$  decay of the giant dipole resonance. The reaction  $^{40}\text{Ca} + ^{40}\text{Ca}$  at  $E_{\text{beam}} = 136$  MeV was used to form the compound nucleus in the isospin  $I = 0$  channel, while the reaction  $^{37}\text{Cl} + ^{44}\text{Ca}$  at  $E_{\text{beam}} = 95$  MeV was used as the reference reaction. The  $\gamma$  rays were detected with the AGATA demonstrator array coupled with  $\text{LaBr}_3:\text{Ce}$  detectors. The temperature dependence of the isospin mixing was obtained and the zero-temperature value deduced. The isospin-symmetry-breaking correction  $\delta_C$  used for the Fermi superallowed transitions was extracted and found to be consistent with  $\beta$ -decay data.

DOI: [10.1103/PhysRevLett.115.222502](https://doi.org/10.1103/PhysRevLett.115.222502)

PACS numbers: 24.30.Cz, 24.60.Dr, 24.80.+y, 25.70.Gh

Symmetries in a complex physical system play a key role for describing it in simple terms and understanding its behavior. In nuclei, the isospin symmetry is based on the experimental evidence of the charge independence of the nuclear interaction. Coulomb interaction breaks isospin symmetry, inducing impurities in the wave functions which affect properties of  $\beta$  decay [1,2] and of the isobaric analogue state (IAS) [3].

In the case of  $\beta$  decay, involving the up ( $u$ ) and down ( $d$ ) quarks, lifetime measurements are used to extract the coupling among these quarks described by the Cabibbo-Kobayashi-Maskawa (CKM) theory. The most precise value of the first term of the CKM matrix  $V_{ud}$  is extracted from the  $ft$  values of  $0^+ \rightarrow 0^+$  superallowed Fermi  $\beta$  decays with several small corrections. One of these corrections,  $\delta_C$ , depends on the isospin mixing [1,2].

Particular effort is being made to deduce the value of isospin mixing for nuclei in different mass regions [4,5]. Tools are selection rules for the electric dipole ( $E1$ )

transition in self-conjugate nuclei [6] and the  $\beta$  Fermi transition between states with different isospin [7].

For the  $E1$  transitions the giant dipole resonance (GDR), where the maximum  $E1$  strength is concentrated, is ideal for searching for small effects in the breaking of the associated selection rule [8–10]. For  $N = Z$  nuclei with medium mass, being not stable, the approach that can be used is to form, via fusion reactions, compound nuclei (CN) with  $N = Z$  at finite temperature ( $T$ ) and then deduce isospin mixing at  $T = 0$  using the model of [11] connecting this quantity from  $T = 0$  to finite  $T$ .

The GDR in nuclei at finite  $T$  and angular momentum was investigated in many experimental and theoretical works and, thus, a solid base exists for the use of this approach [12,13]. For a self-conjugate projectile and target, one ensures that the CN has isospin  $I = 0$ . In this case, the  $E1$  decay of the GDR is hindered because  $I = 1$  states, much less numerous, must be populated [8]. Conversely, if the initial state contains an admixture of  $I = 1$  states, it can

decay to the more numerous  $I = 0$  final states. Thus, the first-step  $\gamma$  yield depends on the degree of isospin mixing of the CN. At finite  $T$  one expects a partial restoration of the isospin symmetry because the degree of mixing in a CN is limited by its finite lifetime, as predicted by Wilkinson [14].

In Ref. [15] the isospin mixing was investigated at  $N = Z = 40$  at  $T = 3$  MeV, while previous works concern CN with smaller  $N = Z$  values only. The work on  $^{80}\text{Zr}$  [15] showed that by using the latest prediction of the isospin mixing value (based on EDF models [16]) together with the expression giving the  $T$  dependence of the isospin mixing [11], one finds a good agreement with the measured value at  $T = 3$  MeV. This finding indicates that with an additional experimental point at another  $T$  one could deduce, from the combined data analysis, the value at  $T = 0$ . The additional point should be at  $T < 3$  MeV to check the predicted trend of the  $T$  dependence of the isospin mixing. This type of analysis will provide a stringent test to model predictions [16].

In this Letter we report on a new study at  $T \approx 2$  MeV addressing the problem of isospin mixing in  $Z = N = 40$ , for which, for the first time, the different residual nuclei were also measured. The aim is to make a combined analysis of this new datum with the previous one at  $T \approx 3$  MeV, in order to (i) test the trend of the  $T$  dependence of isospin mixing, (ii) extract for the first time the value of the isospin mixing for  $Z = 40$  at  $T = 0$ , and (iii) extract, for the first time, the isospin mixing correction  $\delta_C$  necessary to obtain the correct  $ft$  value of superallowed Fermi transitions.

The experiment was performed at the laboratory LNL (INFN, Italy) employing beams from the TANDEM accelerator. Two fusion reactions were used: one was  $^{40}\text{Ca} + ^{40}\text{Ca}$  at  $E_{\text{beam}} = 136$  MeV symmetric in target and projectile, forming the  $^{80}\text{Zr}$  CN with  $E^* = 54$  at isospin  $I = 0$ , the other was  $^{37}\text{Cl} + ^{44}\text{Ca}$  at  $E_{\text{beam}} = 95$  MeV asymmetric in target and projectile, forming the  $^{81}\text{Rb}$  CN at  $E^* = 54$  at  $I \neq 0$ . It is important, in fact, to have a reference reaction not affected by isospin mixing.

The temperature of the CN on which the GDR is built was deduced as  $T = \sqrt{(E^* - E_{\text{GDR}} - E_{\text{rot}})/a}$  where  $E_{\text{GDR}}$  is the GDR energy,  $E_{\text{rot}}$  is the rotational energy, and  $a = A/8 \text{ MeV}^{-1}$  is the level density parameter and  $A$  the mass number.

The experimental setup consisted of the AGATA Demonstrator [17] array coupled to the HECTOR<sup>+</sup> [18] array. AGATA consisted of four triple clusters of segmented HPGe detectors which were used to measure low-energy  $\gamma$  rays. The HECTOR<sup>+</sup> array consisted of seven large volume  $\text{LaBr}_3:\text{Ce}$  with good efficiency up to 20 MeV.

The data analysis used the statistical model and was mainly based on three steps: (i) the first consists of the best possible check of the statistical model in predicting residual nuclei; (ii) the second concerns the analysis of the  $^{81}\text{Rb}$  spectrum to deduce the GDR parameters; and (iii) the last consists of the analysis of the  $^{80}\text{Zr}$  spectrum to deduce the isospin mixing as the only free parameter.

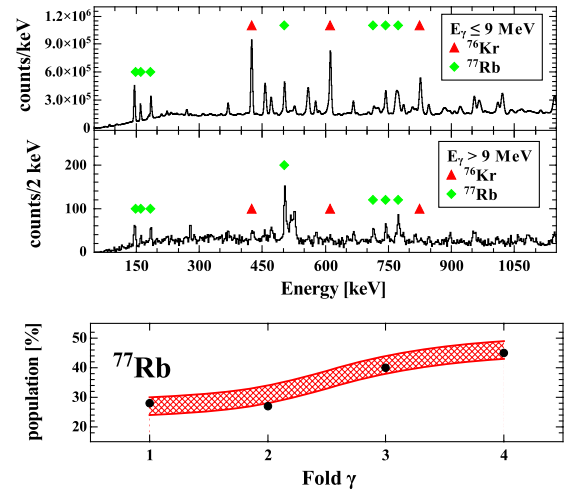


FIG. 1 (color online). Top:  $\gamma$ -ray energy spectra from the decay of the  $^{80}\text{Zr}$  for two different conditions on  $\text{LaBr}_3:\text{Ce}$ . The  $\gamma$  transitions of two residues are indicated with triangles and diamonds. Bottom: Population of the  $^{77}\text{Rb}$  residue versus the measured fold of  $\gamma$ -ray coincidences. Experimental values are displayed with filled circles while red lines are the statistical model predictions. The dashed area was obtained by varying the level density parameter from 7.5 to 8.5. The lower (upper) limit corresponds to  $k = 7.5$  (8.5).

The used statistical model was found to describe, in general, rather well the population of residual nuclei. This was deduced from  $\gamma$ -ray intensities for different gating conditions on high-energy  $\gamma$  rays. The top panels of Fig. 1 show the  $\gamma$ -ray spectra from AGATA in coincidence with  $\gamma$  rays detected with  $\text{LaBr}_3:\text{Ce}$ 's ( $< 9$  MeV for the top panel and  $> 9$  MeV for the middle panel). One sees that the residual nucleus  $^{77}\text{Rb}$  (three protons emission) is more strongly populated in coincidence with a  $\gamma$  ray in the GDR region ( $> 9$  MeV) while the  $^{76}\text{Kr}$  nucleus (four protons emission) is weakly populated when a GDR  $\gamma$  ray is emitted. This reflects the population of different regions of the phase space. In general, the three most strongly populated residual nuclei ( $^{76}\text{Kr}$ ,  $^{74}\text{Kr}$ , and  $^{77}\text{Rb}$ ) are found to be rather well reproduced by the statistical model. Another stringent test is the comparison between data and predictions for the population of specific residual nuclei as a function of coincidence fold, after corrections for the simulated response function. The bottom panel of Fig. 1 shows this comparison for  $^{77}\text{Rb}$ . The error band was obtained by varying the level density parameter  $a$  ( $a = A/k \text{ MeV}^{-1}$  and  $k$  was varied from 7.5 to 8.5), since this is an important quantity for the calculation of the GDR  $\gamma$  decay.

The high-energy  $\gamma$ -ray spectra measured with the  $\text{LaBr}_3:\text{Ce}$  scintillators are shown in Fig. 2. They were analyzed with the statistical model and the corresponding calculations (folded with the detector response function and normalized to the data at around 5 MeV) were obtained with the CASCADE code [19,20] version

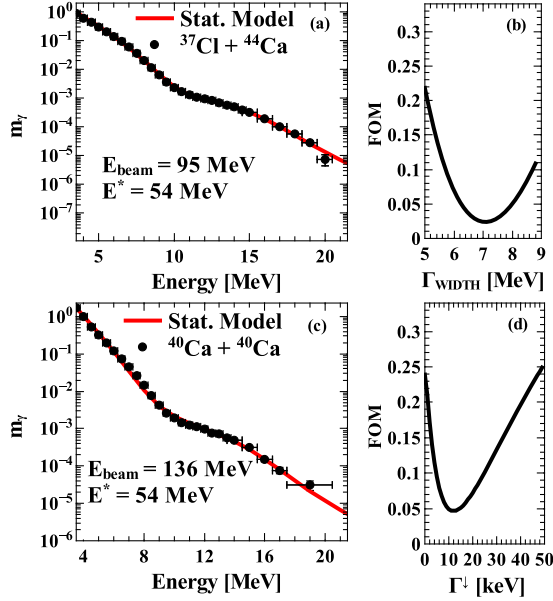


FIG. 2 (color online). Left: High-energy  $\gamma$ -ray spectra for the reactions  $^{37}\text{Cl} + ^{44}\text{Ca}$  (a) and  $^{40}\text{Ca} + ^{40}\text{Ca}$  (c). The data, measured with  $\text{LaBr}_3:\text{Ce}$  detectors, are shown with full circles in comparison with the best-fitting statistical model calculations (red lines). Right: Figure of merit (FOM) obtained by varying the GDR width for  $^{37}\text{Cl} + ^{44}\text{Ca}$  (b) and by varying the Coulomb spreading width for  $^{40}\text{Ca} + ^{40}\text{Ca}$  (d). The FOM is the  $\chi^2$  divided by the number of counts.

including the isospin formalism (as in Ref. [15]). The analysis of the spectrum for the  $^{81}\text{Rb}$  compound nucleus provided the GDR parameters as derived from the best fit to the data in the region between 8 and 15 MeV. Because of the exponential nature of the spectra, the fit minimization was applied to a figure of merit (FOM) obtained dividing the standard  $\chi^2$  over the number of counts, to increase the sensitivity to the low yield part of the spectra [12]. For  $^{81}\text{Rb}$  the best-fitting values (see the corresponding FOM in the top right-hand panel of Fig. 2) for the centroid, width, and strength of GDR were found to be  $E_{\text{GDR}} = 16.4 \pm 0.2 \text{ MeV}$ ,  $\Gamma_{\text{GDR}} = 7.0 \pm 0.2 \text{ MeV}$ , and  $S_{\text{GDR}} = 0.90 \pm 0.05$ , in agreement with the systematics and liquid drop model calculations [15,21].

For the statistical model analysis of the spectrum associated with  $^{80}\text{Zr}$ , the isospin mixing plays a role while all the other parameters were fixed from the  $^{81}\text{Rb}$  analysis. The isospin mixing is included in the code according to the model in Ref. [22] in which the mixing between the state  $I_{<} = I_0$  and  $I_{>} = I_0 + 1$  is considered, where  $I_0$  is the initial CN state. These states exhibit, at high excitation energy, a decay width  $\Gamma_{\gtrless}^{\uparrow}$  and the mixing probability  $\alpha_{\gtrless}^2$  of states  $\gtrless$  in states  $\lesseqgtr$  that can be defined as:

$$\alpha_{\gtrless}^2 = \frac{\Gamma_{\gtrless}^{\downarrow}/\Gamma_{\gtrless}^{\uparrow}}{1 + \Gamma_{\gtrless}^{\downarrow}/\Gamma_{\gtrless}^{\uparrow} + \Gamma_{\lesseqgtr}^{\downarrow}/\Gamma_{\lesseqgtr}^{\uparrow}}. \quad (1)$$

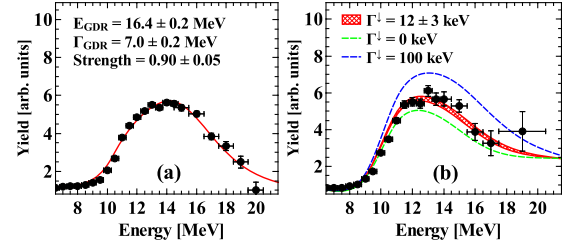


FIG. 3 (color online). Linearized measured and calculated  $\gamma$ -ray spectra for  $^{37}\text{Cl} + ^{44}\text{Ca}$  (a) and for  $^{40}\text{Ca} + ^{40}\text{Ca}$  (b) in the GDR region. In (b) the statistical model calculations are shown corresponding to different values of the Coulomb spreading width:  $\Gamma_{>}^{\downarrow} = 12 \pm 3 \text{ keV}$  (red line), for no mixing  $\Gamma_{>}^{\downarrow} = 0 \text{ keV}$  (green dashed line), and for full mixing  $\Gamma_{>}^{\downarrow} = 100 \text{ keV}$  (blue dashed line).

The mixing probability  $\alpha_{\gtrless}^2$  of states depends on the Coulomb spreading width  $\Gamma_{\gtrless}^{\downarrow}$  of the states  $\gtrless$ . A partial restoration of isospin symmetry at high excitation energy is expected because  $\Gamma_{>}^{\downarrow}$  is rather constant along with the excitation energy while  $\Gamma_{>}^{\uparrow}$  increases rapidly.

To extract the isospin mixing in  $^{80}\text{Zr}$ , the Coulomb spreading width was treated as the only free parameter to fit the  $^{80}\text{Zr}$  data. The best fit of the  $^{80}\text{Zr}$  data was obtained when the Coulomb spreading width is equal to  $\Gamma_{>}^{\downarrow} = 12 \pm 3 \text{ keV}$  (the error includes statistical and GDR parameter uncertainties). The plot of the corresponding FOM is shown in the bottom right-hand panel of Fig. 2. Note that the major contribution to the FOM values comes from the 10–17 MeV region of the spectrum. Indeed (see, e.g., Ref. [23]), the  $\gamma$  yield at different energy intervals originates from different regions of the phase space sampled by the deexcitation cascades. The  $\gamma$  yield at  $E^* < 9 \text{ MeV}$  is mainly due to emission at the end of the deexcitation process after neutron and proton evaporation and thus has lost information on the isospin initial condition. Only the region of the GDR, before proton and neutron emission, is sensitive to the selection rule for  $E1$  decay.

To emphasize the data in the GDR region and the isospin mixing effect, it is important to examine the spectra in a linearized form, given in Fig. 3. These were obtained by dividing the measured and calculated spectra with a statistical model calculation in which the  $B(E1)$  has a constant value, instead of the standard Lorentzian function, (see Fig. 3) [12,15]. To provide a more convincing evidence of the effect of the Coulomb spreading width, calculations were also made assuming full mixing [see the dashed blue line in Fig. 3(b)] and no mixing [see the green dashed line in Fig. 3(b)].

The  $\Gamma_{>}^{\downarrow} = 12 \pm 3$  obtained in this analysis is consistent with the value of  $10 \pm 3$  of Ref. [15] at  $E^* = 84 \text{ MeV}$  and with the value deduced from the IAS width [24] for the ground state of  $^{80}\text{Se}$ . This result confirms, firstly, that the Coulomb spreading width is a quantity rather independent of temperature [22,25] and, secondly, that the Coulomb



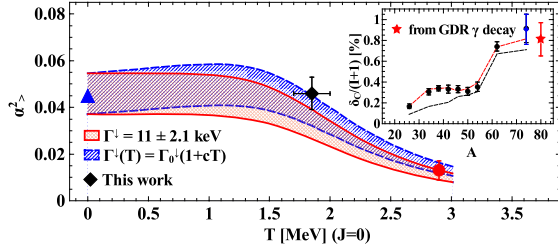


FIG. 4 (color online). The isospin mixing  $\alpha_{>}^2$  as a function of  $T$  obtained with the procedure of Ref. [11] corresponding to  $\Gamma_{>}^{\downarrow} = 11.0 \pm 2.1$  keV (red region), constant with  $T$ . For the blue band,  $\Gamma_{>}^{\downarrow}$  was assumed to vary mildly and linearly with  $T$ . The blue triangle is the theoretical value at  $T = 0$  from Ref. [16], the red circle is the datum from Ref. [15], and the black diamond is the datum of this work. The inset gives the isospin mixing correction  $\delta_C$  as a function of the nuclear mass  $A$ . The black line is the prediction from the Damgaard model [28], while the red line is a shell model with Saxon-Woods radial wave function [29]. Black circles are data extracted from  $\beta$  decay [1], the blue diamond is from the mass measurement [30], and the red star is from this work.

spreading width extracted from the GDR analysis is very similar in size to the IAS width. This indicates that they come from the same physical mechanism [26,27]. Following Ref. [15] and prescriptions of Ref. [11], we express the degree of mixing at angular momentum  $J = 0$  and we obtained a value of  $\alpha_{>}^2 = 4.6\% \pm 0.7\%$ , which is, as expected, significantly larger than the value from Ref. [15] shown in Fig. 4. This supports the concept that the mixing probability is a dynamical mechanism in the nucleus, governed by the lifetime of the system and thus it decreases with the excitation energy.

To compare the two data for  $^{80}\text{Zr}$  at finite  $T$  with the predictions for the ground state, we used the model of Ref. [11], which describes the variation of the mixing probability with  $T$ . The isospin mixing probability for a nucleus at finite temperature is defined as

$$\alpha_{>}^2(T) = \frac{1}{I_0 + 1} \frac{\Gamma_{\text{IAS}}^{\downarrow}}{\Gamma_{\text{CN}}(T) + \Gamma_{\text{IVM}}(\text{IAS})}, \quad (2)$$

where  $\Gamma_{\text{IAS}}^{\downarrow}$  is the Coulomb spreading width of the IAS, to be considered equal to  $\Gamma_{>}^{\downarrow}$ , and  $\Gamma_{\text{IVM}}(\text{IAS})$  is the width of the isovector monopole resonance (IVM) at the excitation energy of the IAS, which is expected to be constant with  $T$ . According to the systematics for the present case, one has  $\Gamma_{\text{IVM}}(\text{IAS}) = 240$  keV [3,11,15].  $\Gamma_{\text{CN}}(T)$  is the CN decay width increasing with  $T$  ( $\Gamma_{\text{CN}} \approx e^{-\Delta E/T}$ , where  $\Delta E$  is the energy removed by the emitted particle). In Fig. 4 the values of  $\alpha_{>}^2$  calculated using Eq. (2) are shown as a function of  $T$ . The red line is obtained with a value of  $\Gamma_{>}^{\downarrow} = 11.0 \pm 2.1$  keV, corresponding to the average of the two experimental values (the lower and upper curves corresponding to 8.9 and 13.1 keV, respectively). This calculation gives at  $T = 0$ ,  $\alpha_{>}^2 = 4.6\% \pm 0.9\%$ , in rather

good agreement with the prediction in Ref. [16]. Following the discussion in Ref. [11], we also considered a weak linear dependence on  $T$  of the Coulomb spreading width given by  $\Gamma_{>}^{\downarrow}(T) = \Gamma_{>}^{\downarrow}(1 + cT)$ . The chosen parameter  $c = 0.1$  MeV $^{-1}$  is such that the value of  $\Gamma_{>}^{\downarrow}$  stays within the experimental error bar. The blue band in Fig. 4 displays the dependence of  $\alpha_{>}^2$  with  $T$  when such weak dependence of  $\Gamma_{>}^{\downarrow}$  is considered (the limiting curves correspond to  $\Gamma_{>}^{\downarrow} = 8.9$  and 13.1 keV). We also performed two calculations using  $\Gamma_{>}^{\downarrow} = 11.0$  keV and  $\Gamma_{\text{IVM}}(\text{IAS}) = 220$  and 260 keV and found that these two curves are well within the two colored bands of Fig. 4.

It is very interesting to connect the isospin mixing parameter  $\alpha_{>}^2$  with the isospin-correction term  $\delta_C$ . As reported in Ref. [31], the quantity  $\delta_C$  is defined as

$$\delta_C = 4(I + 1) \frac{V_1}{41\xi A^{2/3}} \alpha^2, \quad (3)$$

where  $V_1 = 100$  MeV and  $\xi = 3$ , while  $\alpha^2$  is the isospin impurity in the ground state and  $I$  is the isospin of the nucleus. Using Eq. (3), the value  $\delta_C = 0.81\% \pm 0.16\%$  was obtained for  $^{80}\text{Zr}$ . This is shown in the inset of Fig. 4 with calculations from Ref. [1] and other values at lower  $Z$  from  $\beta$  decay [1] and mass measurement [30]. The present result is consistent with data for  $^{74}\text{Rb}$ , and the trend of predictions is also in agreement with the present new point. No calculations of the type of Ref. [1] are available for  $A = 80$ , and the  $\delta_C$  data for  $^{74}\text{Rb}$  are the only existing ones close to  $N = Z = 40$ .

In conclusion, for the first time, the  $T$  dependence of the isospin mixing was obtained for the  $^{80}\text{Zr}$  nucleus, the heaviest that can be formed with stable nuclei. The  $T = 0$  value was deduced and provides a stringent test to theory. The isospin-correction term used in the  $\beta$ -decay analysis was also extracted for the first time for  $A = 80$  and found to be consistent with systematics from  $\beta$ -decay and mass measurements. This result supports the validity of the method based on the GDR at finite  $T$  to obtain isospin mixing in regions of  $Z$  not directly accessible at  $T = 0$ .

The authors wish to thank P. F. Bortignon and H. Sagawa. This work was supported by PRIN No. 2001024324\_01302, the Polish National Center for Science Grants No. 2013/08/M/ST2/00591 and No. 2011/03/B/ST2/01894, and the Spanish Grant No. FPA2011-29854-C04-01. German Bundesministerium für Bildung und Forschung (BMBF) under Contract No. 05P12PKFNE TP4.

\*Present address: RIKEN Nishina Center, 2-1 Hirosawa, Wako, 351-0198 Saitama, Japan.

- [1] I. S. Towner and J. C. Hardy, *Phys. Rev. C* **82**, 065501 (2010).
- [2] W. Satuła, J. Dobaczewski, W. Nazarewicz, and M. Rafalski, *Phys. Rev. Lett.* **106**, 132502 (2011).

- [3] T. Suzuki, H. Sagawa, and G. Colo, *Phys. Rev. C* **54**, 2954 (1996).
- [4] M. A. Bentley and S. M. Lenzi, *Prog. Part. Nucl. Phys.* **59**, 497 (2007).
- [5] D. D. Warner, M. A. Bentley, and P. Van Isacker, *Nat. Phys.* **2**, 311 (2006).
- [6] E. Farnea *et al.*, *Phys. Lett. B* **551**, 56 (2003).
- [7] N. Severijns *et al.*, *Phys. Rev. C* **71**, 064310 (2005).
- [8] J. A. Behr, K. A. Snover, C. A. Gossett, M. Kicińska-Habior, J. H. Gundlach, Z. M. Drebi, M. S. Kaplan, and D. P. Wells, *Phys. Rev. Lett.* **70**, 3201 (1993).
- [9] M. N. Harakeh, D. H. Dowell, G. Feldman, E. F. Garman, R. Loveman, J. L. Osborne, and K. A. Snover, *Phys. Lett. B* **176**, 297 (1986).
- [10] M. Kicińska-Habior, E. Wójcik, O. Kijewska, M. Kisieliński, M. Kowalczyk, and J. Choiński, *Nucl. Phys. A* **731**, 138 (2004).
- [11] H. Sagawa, P. F. Bortignon, and G. Colò, *Phys. Lett. B* **444**, 1 (1998); private communication.
- [12] O. Wieland *et al.*, *Phys. Rev. Lett.* **97**, 012501 (2006).
- [13] A. Bracco, F. Camera, M. Mattiuzzi, B. Million, M. Pignanelli, J. J. Gaardhøje, A. Maj, T. Ramsøy, T. Tveter, and Z. Żelazny, *Phys. Rev. Lett.* **74**, 3748 (1995).
- [14] D. H. Wilkinson, *Philos. Mag.* **1**, 379 (1956).
- [15] A. Corsi *et al.*, *Phys. Rev. C* **84**, 041304(R) (2011).
- [16] W. Satuła, J. Dobaczewski, W. Nazarewicz, and M. Rafalski, *Phys. Rev. Lett.* **103**, 012502 (2009).
- [17] S. Akkoyun, AGATA Collaboration, *Nucl. Instrum. Methods Phys. Res., Sect. A* **668**, 26 (2012).
- [18] A. Giaz *et al.*, *Nucl. Instrum. Methods Phys. Res., Sect. A* **729**, 910 (2013).
- [19] F. Pühlhofer, *Nucl. Phys. A* **280**, 267 (1977).
- [20] I. Diószegi, *Phys. Rev. C* **64**, 019801 (2001).
- [21] B. L. Berman and S. C. Fultz, *Rev. Mod. Phys.* **47**, 713 (1975).
- [22] H. L. Harney, A. Ritcher, and H. A. Weidenmüller, *Rev. Mod. Phys.* **58**, 607 (1986).
- [23] J. J. Gaardhøje, O. Andersen, R. M. Diamond, C. Ellegaard, L. Grodzins, B. Herskind, Z. Sujkowski, and P. M. Walker, *Phys. Lett. B* **139B**, 273 (1984).
- [24] S. Kailas, S. Saini, M. K. Mehta, N. Veerabahu, Y. P. Viyogi, and N. K. Ganguly, *Nucl. Phys. A* **315**, 157 (1979).
- [25] E. Kuhlmann, *Phys. Rev. C* **20**, 415 (1979).
- [26] J. Jänecke, M. N. Harakeh, and S. Y. Van der Werf, *Nucl. Phys. A* **463**, 571 (1987).
- [27] G. Colo, M. A. Nagarajan, P. Van Isacker, and A. Vitturi, *Phys. Rev. C* **52**, R1175 (1995).
- [28] J. Damgaard, *Nucl. Phys. A* **130**, 233 (1969).
- [29] I. S. Towner, J. C. Hardy, and M. Harvey, *Nucl. Phys. A* **284**, 269 (1977).
- [30] A. Kellerbauer *et al.*, *Phys. Rev. Lett.* **93**, 072502 (2004).
- [31] N. Auerbach, *Phys. Rev. C* **79**, 035502 (2009).